NeuroImage 265 (2023) 119778

Contents lists available at ScienceDirect

NeuroImage

journal homepage: www.elsevier.com/locate/neuroimage

Concurrent contextual and time-distant mnemonic information co-exist as feedback in the human visual cortex

Javier Ortiz-Tudela[a,*], Johanna Bergmann[b], Matthew Bennett[c], Isabelle Ehrlich[a], Lars Muckli[d], Yee Lee Shing[a,e,f,*]

[a] Department of Psychology, Goethe University Frankfurt, Frankfurt am Main, Hessen, Germany
[b] Max Planck Institute for Human Cognitive and Brain Sciences, Leipzig, Germany
[c] Université Catholique de Louvain, Louvain-la-Neuve, Belgium
[d] School of Psychology and of Neuroscience, University of Glasgow, United Kingdom
[e] IDeA Center for Individual Development and Adaptive Education, Frankfurt am Main, Germany
[f] Brain Imaging Center, Goethe University Frankfurt, Frankfurt am Main, Germany

ARTICLE INFO

Keywords:
Predictive processing
Feedback signals
Vision
Episodic
Semantic
Retrieval

ABSTRACT

Efficient processing of the visual environment necessitates the integration of incoming sensory evidence with concurrent contextual inputs and mnemonic content from our past experiences. To examine how this integration takes place in the brain, we isolated different types of feedback signals from the neural patterns of non-stimulated areas of the early visual cortex in humans (i.e., V1 and V2). Using multivariate pattern analysis, we showed that both contextual and time-distant information, coexist in V1 and V2 as feedback signals. In addition, we found that the extent to which mnemonic information is reinstated in V1 and V2 depends on whether the information is retrieved episodically or semantically. Critically, this reinstatement was independent on the retrieval route in the object-selective cortex. These results demonstrate that our early visual processing contains not just direct and indirect information from the visual surrounding, but also memory-based predictions.

1. Introduction

Successful navigation through our world requires the efficient integration of sensory inputs with existing knowledge. The predictive processing framework (Clark, 2013; Friston, 2005; Rao and Ballard, 1999a) explains how this integration could take place within the visual domain in the context of a hierarchically organized system. Within this framework, pre-existing knowledge exerts its influence in the form of top-down (i.e., feedback) signals sent from higher to lower levels in the hierarchy (with "feedback" denoting the directionality of the underlying anatomical connections); these signals are then contrasted against incoming (i.e., feedforward) information initiated at the retinas. However, to what extent feedback signals represent only low-level visual features of neighbouring locations (e.g., extensions of lines) or also features drawn from higher-level knowledge about expected scene content (e.g., objects typically found in a scene) is not still fully understood. A full characterization of the content in feedback signals, understood as the top-down requires their decomposition into at least two types of information, namely, concurrent and mnemonic (Fig. 1). *Concurrent* refers to information about the contextual surrounding of a given stimulus (Fig. 1, red portion). This type of information aids visual processing by providing features from the context that can inform less detailed inputs, such as poorly illuminated or partially occluded objects (Bar, 2004). In contrast, *mnemonic* denotes information that is no longer available from the environment, but which may be retrieved internally. One of the main candidate mechanisms for providing time-distant content is memory retrieval. Indeed, if a memory trace is retrieved (e.g., from a previous visit to a place; Fig. 1, blue cloud), information stored in that trace can be sent down to perceptual regions and help to disambiguate the percept based on previous knowledge (Bar, 2004; Friston, 2005). However, the precision of this disambiguation could depend on the nature of the information that is retrieved and on the neural substrates recruited to do so. On the one hand, episodic memories, defined as information about past experiences that is bound to a specific spatio-temporal context, are assumed to be rich in perceptual details from the event that generated the episode (e.g., your breakfast this morning; (Squire, 1998; Tulving, 1985)) and to rely critically on parietal and medial temporal structures (Ritchey and Cooper, 2020; Tulving and Markowitsch, 1998). On the other hand, semantic memories reflect generalized real-world knowledge acquired through a life-long set of experiences and convey more abstract information (e.g., the general concept of breakfast; (Squire, 1998; Tulving, 1985)). Accessing these latter

* Corresponding authors at: Department of Psychology, Goethe University Frankfurt, Frankfurt am Main, Hessen, Germany.
E-mail addresses: ortiztudela@psych.uni-frankfurt.de (J. Ortiz-Tudela), shing@psych.uni-frankfurt.de (Y.L. Shing).

https://doi.org/10.1016/j.neuroimage.2022.119778.
Received 30 September 2022; Received in revised form 14 November 2022; Accepted 29 November 2022
Available online 30 November 2022.

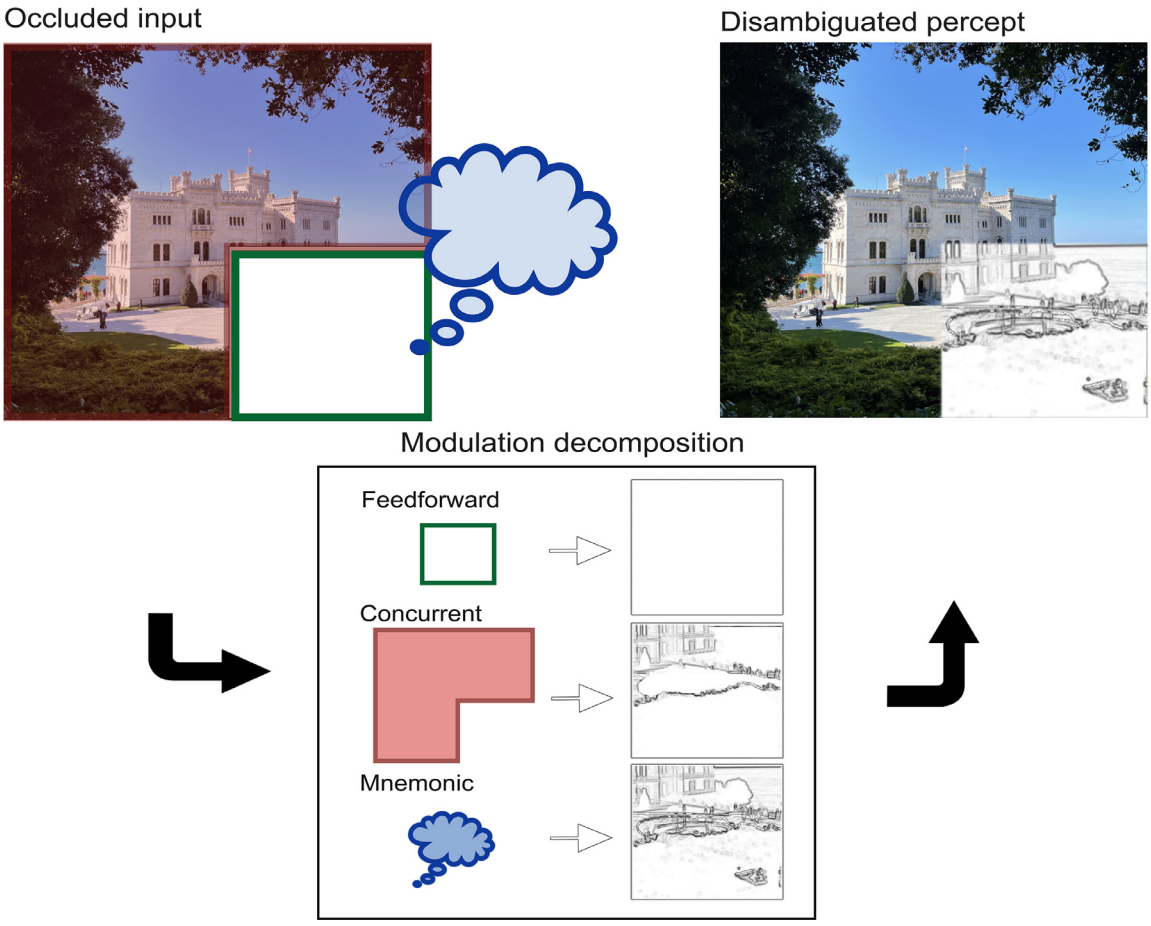

Fig. 1. Schematic decomposition of the modulation of activity in occluded EVC areas. This schematic shows the hypothesized origins of information fed to brain regions with receptive fields located in the occluded, bottom right corner of the image. Green: activity is predominantly modulated by direct sensory information from the eyes (i.e., feedforward information). In this example, it would be uninformative white light. Red: content that is concurrently reaching other visual regions (i.e., concurrent information) biases activity via lateral connections by providing contextual information. In the example picture, this would be the edges of the building, the sea behind it, and the bushes and ground in front of the building. Blue: time-distant information that is not currently presented but that can be accessed through memory (i.e., mnemonic information) can provide further details from previous encounters. In the example picture this would be a memory from the fountain at the Miramare Castle (Trieste). These three sources of modulation jointly contribute to perceptual disambiguation.

representations involves a much more distributed network of multimodal regions including posterior (e.g., inferior parietal lobe, middle temporal gyrus and fusiform cortex), medial (e.g., parahippocampal gyri and posterior cingulate gyrus) and prefrontal (e.g., dorso- and ventromedial prefrontal cortex) regions (Binder et al., 2009). In spite of their potential to serve as sources of content for visual processing, so far, no study has directly compared episodic and semantic retrievals as potential mechanisms through which the information serves as feedback in the brain.

In the current study, we combined partial occlusion with a memory task to characterize the content of feedback signals in the early visual cortex (EVC). More specifically, we intended to 1) isolate separate contributions of concurrent and mnemonic information to feedback signals and 2) to assess the extent to which the mnemonic contribution differs depending on whether the information is accessed episodically or semantically. To do so, we recorded brain activity from a group of human participants while they were exposed to a set of room images. The images were overlaid with a white rectangular patch covering the bottom-right corner and the centre of the images; critically, the occluder hid a target object (Fig. 2A). Participants were instructed to mentally represent the entire room including the target object behind the occluder without moving their eyes from the centre of the screen. This setup, akin to those used in the mental imagery literature (Albers et al., 2013; Kosslyn and Thompson, 2003), allowed us to track the representation of the target objects without ever showing them inside the scanner. The target object for each room was non-ambiguous, and could be accessed either entirely episodically (i.e., based on associative memory of object-room pairings that were studied the day before) or relatively more semantically (i.e., no associative memory, rather using their real-world knowledge to retrieve the specific object that fits the room). See Fig. S1 for participants' training performance of the object-room associative memory and *Supplementary Text* for more details. Using functional retinotopy and field-of-view mapping, we identified brain voxels in V1 and V2 that represented the portion of the visual field where the white patch was placed. By doing so, we isolated activity patterns from non-stimulated regions of the visual cortex where the target objects were mentally placed (see Smith and Muckli 2010, for a similar approach). We used multivariate pattern analysis to decode concurrent and mnemonic content from these non-stimulated voxels. In addition, we assessed whether the representation of mnemonic content in these voxels depended on the target object being accessed based on associative episodic memory or semantic knowledge of the object. Finally, to ascertain the involvement of non-visual regions in our task, we performed a whole-brain psychophysiological interaction (PPI) analysis to identify

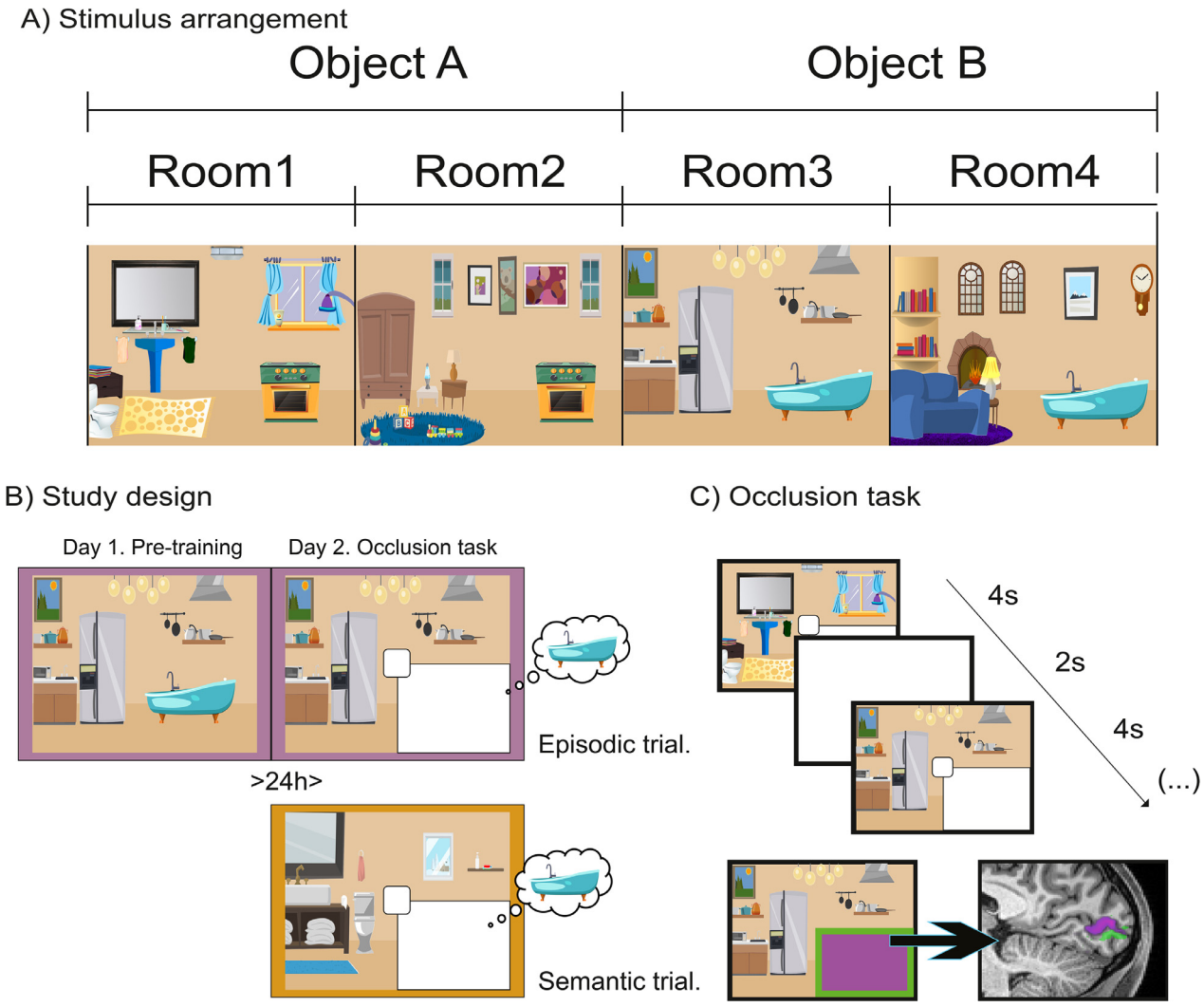

Fig. 2. Basic experimental schematics. (A) Four example trials. Each object was assigned to two different rooms for each memory condition. (B) Experimental paradigm. On episodic trials participants retrieved the object studied on day 1; on semantic trials participants retrieved the object that would semantically fit the room (C) Occlusion task. Top panel: Participants were shown a sequence of flickering rooms with one occluded quadrant. Bottom panel: Field of view mapping was used to isolate voxels responding to the occluded region (purple); voxels with receptive fields close to the edge of the occluded region (green) were removed from the analysis.

changes in effective connectivity between early visual regions and the rest of the brain as a function of task condition.

2. Materials and methods

2.1. Registration

Prior to data collection, a registration was created and is available at https://osf.io/va6fc; deviations from this registration are indicated in the corresponding sections.

2.2. Participants

The initial targeted sample size of forty participants had to be adjusted due to the COVID-19 pandemic. Thirty healthy young adults were recruited through advertisements placed across the three campi of the Goethe University in Frankfurt. They all gave written informed consent to participate in this study, in accordance with the Ethics Committee FB05 of the Goethe University (Protocol number: 2019-38). In exchange for participation, they received either course credits (for Psychology majors) or honorarium (for all other majors). All participants had normal or corrected-to-normal vision. One of the participants had to be excluded due to excessive movement during three out of the four functional runs in the scanning session. Thus, the final sample size was twenty-nine (18 female; age: mean = 22.61, sd = 2.12).

2.3. Stimuli and materials

Previous studies using partially occluded images have used real-world photographs as stimuli (Morgan et al., 2016, 2019; Smith and Muckli, 2010). When using this kind of stimuli, the location of the occluder bears no relation to the structure of the image content itself, thus resulting in seemingly random cuts in the picture. These random cuts generate abrupt stops of lines right at the edge of the occluder (e.g., tree trunks or traffic lights) that randomly vary from photograph to photograph but that are constant for all the repetitions of the same photograph. As a consequence, differences in neural representation between photographs could reflect differences in responses to line stops without the need for any top-down influence. Since one of our goals was to study mnemonic content, we created a novel stimulus set that did not include any meaningful line stop using an online platform (Animaker, 2018).

This set consisted of sixteen cartoon images depicting common indoor locations and four cartoon images of commonly used objects. Importantly, all pictures were adjusted so that the location that the occluder would cover included only one line (i.e., a straight line that separated the floor from the wall) which was held constant across all pictures. All materials are available at https://github.com/ortiztud/feedbes.

Our stimulus set comprised sixteen rooms and four objects. Room images depicted eight indoor locations, namely, kitchen, bathroom, living room, bedroom, kitchen supplies store, electronic store, furniture store and bath supplies store, and two instances of each location were used. Object images depicted an oven, a bathtub, a bed and a tv. The full set was divided into two subsets. For the episodic subset, eight room-object pairs were built so that the two elements had a minimal semantic relation (e.g., "TV" in a "bathroom"). The remaining eight rooms were used for the semantic subset, and they were paired with objects that had a strong semantic relationship (e.g., "oven" in a "kitchen"). Critically, every object was paired with two rooms in each retrieval condition (Fig. 2A). For episodic trials, every participant was assigned to a given combination of objects and rooms. These combinations were counterbalanced across participants so that across the entire sample every object was seen in every possible room. Counterbalancing was only possible for episodic trials since the real-world association between rooms and objects was 1:1. In order to maximize the differences between episodic and semantic retrievals, rooms and objects were chosen so that each object was uniquely associated with one room. For instance, the “bathtub” for which the “bathroom” was chosen as its associated semantic pair, would not semantically fit in any of the other rooms (i.e., bedroom, kitchen and living room). This arrangement not only ensured the accuracy of the semantic retrievals but also avoided semantic influence in episodic retrievals. Namely, since all episodic combinations were semantically incongruent (e.g., “bathtub” in “kitchen”), the only retrieval route through which participants could access the object was episodic in nature. We, therefore, exploited semantic congruity to increase the relative weight of episodic and semantic components in our two corresponding retrieval conditions. Of course, in real-world settings, episodic retrievals can also be performed on semantically congruent memories, but for the sake of orthogonalization of our conditions, we restricted episodic retrievals to incongruent associations.

During the tasks outside the scanner, stimuli were displayed using a 60 Hz monitor (resolution: 1680 x 1050, full HD) placed approximately 60cm away from participants’ heads. During the tasks inside the scanner, stimuli were displayed using a 60 Hz monitor (resolution 1920 x 1080, full HD) placed 162cm away from participants’ eye (eye to mirror + mirror to monitor distance). Stimuli spanned 16.4º x 12.1º of visual angle.

2.4. Procedure

2.4.1. Day 1

Learning phase (for episodic trials): Participants were presented with five learning blocks during which the pairs from the episodic set were shown sequentially in a computer screen and repeated ten times. Participants were instructed to memorize as many details as possible from the entire image and to pay special attention to the target object (i.e., the object that was placed on the bottom-right corner of the image). In this learning phase, participants were free to move their eyes so that they could form a rich memory trace of both the room and the objects. At the end of each block, memory about the room-object pairings was tested with two tests. Namely, memory for the object identity was measured with a four-alternative forced choice test with the room as cue and the four objects as options; memory for the precise object position was measured by presenting the object misplaced (+/- 100 pixels either horizontally or vertically) and asking participants to place it back into its original position using the arrow keys in the keyboard. The displacement of the objects was randomly chosen from either +100 or -100 pixels either vertically or horizontally so that even with the displacement, the object never fell outside the to-be-occluded region. Note that these displacements were perceived as very small and difficult to notice, and they were included to prompt participants to pay attention to details of the room-object combination. After completing the learning blocks, participants were given a printed version of the images with a white patch occluding the target area and they were asked to draw the target objects from memory. The between-blocks memory tests and the drawing task were included here to ensure that participants formed distinctive and detail-rich memories (e.g., spatial precision, colour palette, texture patterns, etc.) for each pair.

After the learning phase, participants performed one block of the occlusion task (equivalent to one scanning run; see below) to familiarize themselves with the timing and structure of the scanner task. The only difference between this familiarization block and the scanner blocks is that a trial-by-trial ef rating was performed to further promote the rich mental visualization of the objects. On every trial, participants were asked to report their subjective vividness of the retrieved object on a four-point Likert scale.

Finally, at the end of the session, one last learning block, identical to those at the beginning, was conducted as a reminder of the studied stimuli.

2.4.2. Day 2 (24h after day 1)

Pre-scan phase: Right before entering the scanner, participants were briefly shown the rooms in the semantic set to familiarize them with the new stimuli. They were asked to remember the objects studied on day 1 and to mentally select the one that would best fit each room (i.e., those that would be typically found in each location in the real world) and to verbally report it. If they selected the wrong object, the correct answer was provided by the experimenter. This only happened once across the entire sample due to a speeded response from one participant. Note that the actual objects were never shown together with these rooms.

Scanning phase: In order to avoid fatigue and to reduce unwanted movements, we distributed our scanning sequences over two sessions (~50 min each) with a break of roughly 10 min in between; participants were allowed to use the toilet, stretch and walk to prevent neck and shoulders stiffness. Both scanning sessions included one T1 weighted anatomical image, two object retrieval runs and one visual mapping run. In addition, the first session included a high-resolution scan of the hippocampal area and an extra visual mapping run, and the second session included an extra functional run not used for the current project.

2.4.3. Occlusion task

This task consisted of two types of trials: episodic and semantic. On episodic trials, participants were presented with the rooms studied during the learning phase on day 1; on semantic trials, participants were presented with a new set of rooms, which were first introduced on day 2 pre-scan phase. In both trial types, a white patch occluded the bottom right corner of the image, thus hiding the target object and another smaller patch hid the foveal region (see *Target mapping* section below). For each room, participants’ task was to mentally select the corresponding object and to vividly retrieve it. When presented with a “studied” room, participants were asked to access the room-object pairs from the previous day (i.e., episodic access); when presented with a “not studied” room, participants were asked to access the room-object pair that would naturally occur in the real world (i.e., semantic access). Note that only four objects were used in the task and that these were shared between episodic and semantic trials. That is, in both conditions participants had to access the same objects but through different operations (i.e., through episodic retrieval of the events on day 1 or through semantic matching of the room category to the object). As a consequence, the exposure of the to-be-retrieved objects was equal for both trial types. Participants were not explicitly cued in advance about the nature of the upcoming trial, but the extensive training on day one made the identification of the images as “studied” or “not studied” trivial. Trial order transitions

were optimized (Spunt, 2016) to allow for maximum separation of trial types.

Each of the sixteen occluded rooms was shown six times over the course of each run and each presentation lasted 4 s with a blank inter-trial interval of 2 s. During the 4 s of the trial, the image flashed at a 5Hz frequency. For the entire duration of the trial a special type of fixation cross was used to minimize eye movements; see below for an extended description of this. The total duration of the task runs was 576s and participants completed four runs. At the beginning of each run, the experimenter reminded participants to maintain fixation and to "vividly retrieve the entire image by thinking about the color of the objects, their patterns or where they were positioned on the screen".

2.4.4. Retinotopic mapping

To map our participants' visual cortex activity to on-screen positions we used standard stimulation procedures of eccentricity and polar angle mapping. For eccentricity mapping, a contrast-reversing checkerboard expanding ring was displayed at the center of the screen; one full cycle of expansion lasted 56 s and a total of 9 cycles were shown. For polar angle mapping, a contrast-reversing checkerboard rotating wedge was presented centered in the screen; the wedge rotated clockwise to cover the entire screen after 64 s for a total of 8 complete rotations.

2.4.5. Target mapping

We used contrast-reversing flashing checkerboards (flashing frequency 5Hz) to functionally locate the voxels in V1 and V2 responding to our target region (i.e., bottom-right corner of the screen). Previous studies have shown that successfully representing peripherally presented objects can recruit foveal voxels (Williams et al., 2008). Since our objects were initially presented peripherally and participants were asked to retrieve them in their original position, we also included a checkerboard patch that spanned 2º of visual angle from the center of the screen to map the foveal region. By also occluding the foveal region, we were able to later test for the recruitment of foveal voxels when representing our target objects. Analysis of the foveal ROIs are not included in the main text for the sake of conciseness but are included in the *Supplementary Text.*

For each to-be-mapped region two checkerboard patterns were used. One of the patterns covered 1º of visual angle along the inner boundaries of the occluded regions directly adjacent to rest of the image; the other pattern covered the remaining region. The final region considered for analysis was therefore always smaller than the occluder patch shown on the screen. This procedure was used to prevent any voxel with receptive fields lying close to the boundaries from entering our analysis and also to guard against potential small misalignments between functional scans (see Smith and Muckli 2010, for a similar approach).

Each pattern was repeated 6 times following a 12s on/12s off block design. A central fixation cross was shown during the entire duration of the task. To ensure fixation, participants were asked to monitor the color of the fixation cross and to press a button every time that it changed color; color changes were randomly presented during the on periods a maximum of three times.

2.4.5. Post-scan phase

Participants performed a memory test (identical to the one in the learning phase) that checked for room-object associations (both for episodic and semantic pairings). In addition, in the case of the episodic trials, we checked for correct positioning of the objects in the image.

2.5. MRI data acquisition

MRI data was acquired using a 3 Tesla MR scanner (SIEMENS Prisma) with a 32-channel head coil at the Brain Imaging Center (BIC) of the Goethe University (Frankfurt, Germany). In both scanning sessions, a 3D anatomical scan (3D MPRAGE; 1 x 1 x 1 mm resolution; iPAT factor: 2) was acquired. In addition, a high-resolution Turbo Spin Echo scan (TSE; 0.4 x 0.4 x 2 mm resolution; TE= 16ms; TR= 6500ms) was acquired during the first session; the 206mm field of view was placed over each participant's hippocampus (HC) by first locating the left HC and aligning the shorter axis of the field of view to the long axis of the HC. Blood oxygen level-dependent (BOLD) signals were measured with an echo-planar imaging sequence (EPI; TE= 38ms; TR= 800ms; resolution= 2 x 2 x 2 mm; MB factor= 8; flip angle= 52º field of view=208 mm; 72 axial slices; phase encoding direction= AP). Finally, two extra sets of 5 volumes of the EPI sequence were acquired in each phase encoding direction to allow for susceptibility distortion correction.

2.6. MRI data processing

2.6.1. Preprocessing

All structural and functional MRI images, apart from the TSE and functional scans from the retinotopic mapping run, were preprocessed using fMRIPREP 20.0.1 (Esteban et al., 2019) and all multivariate analyses were conducted in native non-smoothed space. A boilerplate text released under a CC0 license describing preprocessing details can be found in the *Supplementary Text.* For further information about the pipeline, see fMRIPREP´s documentation. Functional scans from the retinotopic mapping run were slice time corrected, 3D motion corrected and temporally filtered (high-pass filtered at 0.01 Hz and linearly detrended) using Brain Voyager 21.4 for Linux (Brain Innovation).

2.6.2. ROI definitions

A detailed report of the ROI definition can be found in the Supplementary text. In short, functionally delineated V1 and V2 ROIs were obtained using a standard retinotopic mapping procedure. Each of these ROIs was further restricted to include only voxels responding to the central and peripheral occluded portions of the visual field using the target mapping run. In addition, atlas-based ROIs for the ventromedial prefrontal cortex and for the object selective cortex were obtained from Neurosynth (Yarkoni et al., 2011). Note that only the delineated subregions of V1 and V2 were restricted to occlusion and the rest of the masks were used in their entirety. In what follows, we will be interested in testing for different types of information in occluded subregions of central and peripheral V1 and V2. Unless otherwise stated, all the results below pertain to ROIs that respond exclusively to the occluded part of the visual scene (i.e., ROIs which do not receive meaningful feedforward information).

2.6.3. Generalized linear model

For our multivariate analysis, single-trial beta estimates were obtained by modelling BOLD time course with a series of Generalized Linear Models (GLM) using the Least Squares Separate method (Abdulrahman and Henson, 2016; Mumford et al., 2012) with LSS-16 to obtain trial-specific estimates. The GLM for a given trial contained a total of 32 regressors: one for the onset of the trial, 16 regressors for the onsets for the 16 different rooms, 6 regressors for head motion (3 for displacement and 3 for rotation), 3 regressors for global, WM and CSF intensity, and 6 regressors for eye movements (3 for displacement and 3 for rotation; see *Supplementary Materials*). A total of 96 GLMs per run were computed for every participant and only the single-trial estimates were used further.

2.6.4. Multi-voxel pattern analysis

Single-trial beta estimates for each ROI were used to train and test our classifiers using a leave-one-run-out cross-validation scheme and hence using four cross-validation folds, i.e. training on three runs and testing on the left-out run (full summary of results can be seen in Table S1); note that our GLM approach rendered one beta estimate per trial and hence, our leave one-one-run-out procedure effectively held out 96 observations for testing on each cross-validation fold. All classification analyses were performed with The Decoding Toolbox (Hebart et al., 2015) and were carried out separately for episodic and semantic trials.

In order to test for the presence of concurrent information, a set of binary classifiers was trained and tested with different rooms paired with the same objects (e.g., room 1-object A vs room 2-object A). To get a measure of mnemonic information, we tested our classifiers with different rooms paired with different objects (e.g., room 1-object A vs room 2-object B) and tested them on a different subset of rooms that were paired with the same objects as the train set (e.g., room 3-object A vs room 4-object B). Both procedures rendered 12*3 training samples and 12 test samples in each cross-validation fold. The results of the binary classifiers were then averaged to get a single estimate for each participant. Classifier performance was evaluated with bootstrapping in a two steps procedure (Stelzer et al., 2013). Namely, for each participant trial labels were randomly permuted 100 times, and classification accuracy was assessed for each iteration thus creating 29 accuracy distributions of 100 random classifiers each. In a second step, we randomly selected (with replacement) one sample from each participant's null distribution and average them across participants. This second step was repeated 1000 times to create a null distribution of average accuracies at the group-level. Statistical significance was declared when the sample's true average accuracy was larger than the 99.9% of the observations of the null distribution of average accuracies (i.e., $p < .001$).

2.6.5. Representational (dis)similarity analysis

Neural Representational Dissimilarity Matrices (RDMs): Single-trial beta estimates for each run were used to compute a neural RDM (Kriegeskorte et al., 2008a) for each ROI using The Decoding Toolbox (Hebart et al., 2015) and all subsequent analysis were performed with homebrew scripts available at https://github.com/ortiztud/feedbes. RDMs were computed with cross-nobis distance and capture the similarities among the multivoxel patterns in each ROI with higher values indicating less correlation (i.e., more representational distance).

Model correlation and variance partitioning: Two ideal binary RDMs were simulated to predict what the neural RDMs should look like in the presence of concurrent or mnemonic information. For the concurrent model, the *same room-same object* cells contained zeros and the rest of the cells contained ones; for the mnemonic model, all same object cells (i.e., including same room and different room) contained zeros and the rest of the cells contained ones (see Fig. 4). In these model RDMs, zero represents minimal dissimilarity and one represents maximal dissimilarity. Since the resulting model RDMs overlap in their predictions about the same room-same object trials, when computing the neural RDM to object model RDM correlation, those cells were not included. Finally, in order to assess the unique contribution of each model RDM to explaining the ROI RDMs, a variance partitioning method was applied (Legendre, 2008). A group-level RDM was computed by averaging individual RDMs (after normalization) and separate regression models were fit using either each model separately or both models as regressors; then, the unique contribution of each model was computed by subtracting the explained variance (r^2_{Adj}) for the other model in isolation from the estimate of both models combined. Significance testing on the fractions was performed by running 1000 permutations of the columns in the ROI RDM and comparing the resulting distribution with the original value.

2.6.7. Object specific index

To obtain a distance measure for each object, an object-specific reinstatement index was computed for each neural RDM. We assessed the distance across *different room-same object* pairs and subtracted it from the distance across *different room-different object* pairs (see Fig. 5). All distance measures were Fisher-transformed before averaging across trials. For any given pair of rooms, this index reflects the extent to which retrieving the *same object* decreases the representational distance when compared to retrieving a *different object*. The object-specific reinstatement index was averaged across objects to obtain a single value per ROI per participant. Differences from chance performance were evaluated with one-side Wilcoxon tests against zero.

2.7. Psycho-physiological interaction (PPI)

All PPI analyses were conducted with FEAT (FMRI Expert Analysis Tool) Version 6.00, part of FSL (FMRIB's Software Library, www.fmrib.ox.ac.uk/fsl) (Woolrich et al., 2001). Our registered analysis plan for PPI included V1 as seed region; however, since the object reinstatement analysis revealed unequal reinstatement between trial types in EVC ROIs but an equivalent reinstatement in LOC, we run additional PPI analyses with LOC as seed region to enable a fair comparison between conditions. Therefore, we performed four PPI analyses, one for each seed region and each contrast direction of episodic and semantic trials, i.e., PPI-$V1_{EPISEM}$, PPI-$V1_{SEMEPI}$, PPI-LOC_{EPISEM}, and PPI-LOC_{SEMEPI}. Only the LOC results are reported in the main text but see *Supplementary Text* for the originally registered analyses.

In addition to the nuisance regressors that had been described above for the multivariate GLM, our PPI models included three additional regressors. The first regressor (PHYS) represents the physiological signal of the corresponding seed region, the second regressor (PSY) codes for the respective contrast of conditions, and the third regressor (PHYS*PSY) is the interaction between physiological signal and the psychological condition.

2.7.1. PHYS

For every subject and every run, the average timeseries of both seed ROIs was extracted with FSL's function fslmeants. The resulting vector was entered into the corresponding first-level regression model as a regressor that represents the physiological variable.

2.7.2. PSY

In order to partial out any changes in connectivity that might be driven by main effects of the task, we included in all PPI analyses two psychological regression vectors (PSY_A-B and PSY_A+B) for mean-centering purposes. For PPI-$V1_{EPISEM}$ and PPI-LOC_{EPISEM}, PSY_A-B coded episodic trials as 1 and semantic trials as -1, whereas for PPI-$V1_{SEMEPI}$ and PPI-LOC_{SEMEPI} the coding was reversed. PSY_A+B coded both, episodic and semantic trials, as 1. All psychological regressors were convolved with a standard gamma hemodynamic response function (HRF) before they were entered into the PPI models.

2.7.3. PHYS*PSY

The interaction regressor of interest was created by multiplying the demeaned timecourse of the seed region, i.e., PHYS, with the mean-centered psychological vector A-B, i.e., PSY.

All data were high-pass filtered with a cut-off of 100 s. For the first level analysis, three contrasts were specified, i.e. [1 0 0], [0 1 0], and [0 0 1]. All contrasts were computed voxelwise for the four runs (voxel threshold $z > 3.1$). The resulting estimates were passed on to the second level mixed effect analysis (FLAME, FMRIB's Local Analysis of Mixed Effects), to combine the results across runs. Lastly, second level estimates were brought up to the third level between-subjects group analysis, resulting in the final effective connectivity maps. Group level maps were cluster corrected to an alpha value <.05.

3. Results

3.1. Do feedback signals in EVC contain both concurrent and mnemonic information?

Previous studies using occlusions in naturalistic images have relied on linear support vector machine (SVMs) classifiers to successfully decode information surrounding the occluder (Morgan et al., 2019; Muckli et al., 2015; Smith and Muckli, 2010). To validate our novel paradigm and stimulus set, we mimicked previously reported analysis by attempting to decode room category from non-stimulated brain regions (full summary of results can be seen in Table S1). The first set of SVMs classified between different rooms paired with the same objects,

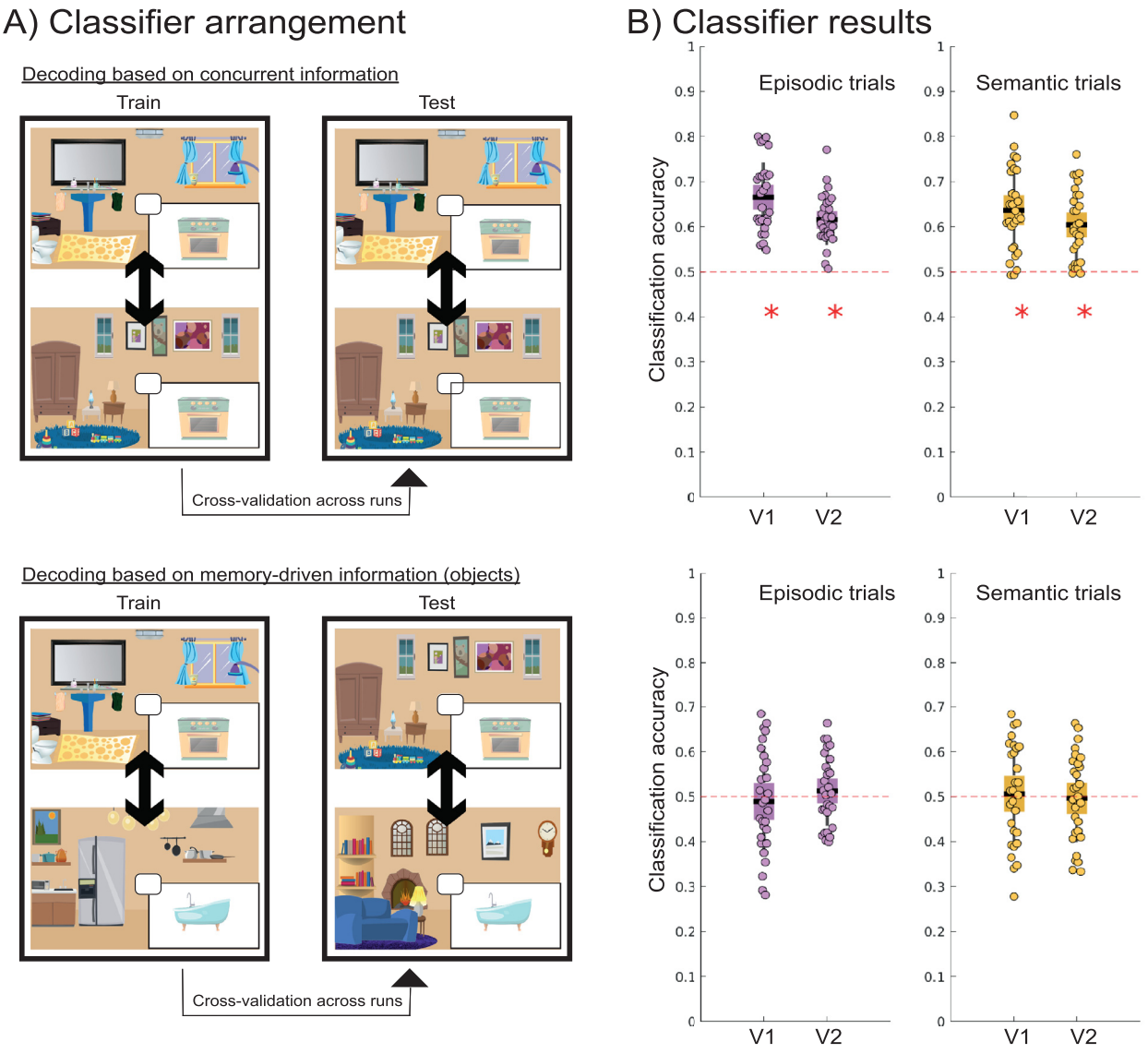

Fig. 3. Classification analysis in functionally delineated EVC ROIs. (A) Classifier arrangement. Two different sets of SVMs were used. The first set classified between different rooms paired with the same objects (top panel) and the second one between different rooms paired with different objects (bottom panel); critically, this second set of SVMs was tested on a different set of rooms that only shared the to-be-remembered object. Note that the objects are only shown here for visualisation purposes and that these were never shown inside the scanner. (B) Cross-validated classification accuracy for concurrent information SVMs (top panel) and mnemonic information SVMs (bottom panel). Each dot represents one participant, and the colour of the box plots denotes the retrieval type (i.e., episodic or semantic). Red asterisks indicate above chance (.50) performance; whiskers represent +-1 standard error of the mean.

such that only the room content (i.e., concurrent information) could differ between classes (Fig. 3A, top panel). Our classifiers performed above chance level (.50) for both episodic and semantic trials (episodic trials: accuracy on V1 = .67 and accuracy on V2 =.62; semantic trials: accuracy on V1=.64 and accuracy on V2 = .60, all ps<.001; Fig. 3B, top panel). This pattern of results replicates and extends previous findings (Morgan et al., 2016, 2019; Smith and Muckli, 2010) by showing that 1) EVC regions that did not receive any meaningful feedforward signals represent surrounding information (i.e., the different rooms), 2) that this pattern is not restricted to real-world pictures but also extends to simplified cartoon stimuli without sudden line stops (see Methods for rationale of creating the stimuli set) and 3) that when memory content is kept constant, concurrent visual information is a constituent part of activity in V1/V2.

In addition to the modulation of EVC activity by concurrent feedback signals, we attempted at finding the effect of memory-driven feedback by classifying between different object retrievals. We set up a cross-classification scheme in which we trained our classifiers in a subset of different room-different object trials (e.g., room1-objectA vs room2-objectB) and tested them in a different subset of trials that maintained the same object association structure (e.g., room3-objectA vs room4-objectB; Fig. 3A, bottom panel). This cross-classification scheme prevented concurrent information from biasing our classifiers performance. In contrast to previous analysis, cross-classification performance did not differ from chance in either memory condition (all p>.05; Fig. 3B, bottom panel), suggesting no memory-related reinstatement which could be generalized between room-object combinations.

The lack of transfer between training and test sets in our cross-classification analysis was unexpected. We reasoned that the decision boundaries learned by our SVMs during the training process might have been driven mostly by concurrent information. If that is the case, our SVMs would not be able to correctly classify mnemonic content in a new set of scenes even if it was present in our ROIs. In order to test this hypothesis, we used Representational (Dis)Similarity Analysis

(Kriegeskorte et al., 2008b), which although it was not initially included in our registered analysis plan, enable the estimation of the relative contributions of each type of information. We computed separate neural RDMs for each ROI in the EVC and created two model RDMs - one for each type of information (Fig. 4A). The model RDM for concurrent information had minimal values in pairs of trials that shared the same room, whereas the model RDM for mnemonic information had minimal values for pairs of trials that shared the same object.

Neural and model RDMs were correlated across ROIs and memory conditions using Spearman's rho (Fig. 4B, top panel). The results revealed a strong correlation between the neural RDMs and the concurrent model for episodic trials (V1rho = .510 and V2rho =.419, both ps<.001) and for semantic trials (V1rho=.511 and V2rho = .416, both ps<.001; Fig. 4B, bottom panel), thus further confirming the previous result from the classification analysis above. More interestingly, the mnemonic model also showed a significant correlation in both ROIs for episodic trials (V1rho = .167 and V2rho =.148, all ps<.001), but not for semantic trials (V1rho=-.06 and V2rho = -.023, all ps>.05). This result suggests that there was in fact memory-driven pattern reinstatement in EVC, but only when object memories were accessed through a purely episodic route with associative memory and not through a route that required semantic knowledge. However, since the correlation with the mnemonic model was weaker than the correlation with the concurrent one, the mnemonic model could be explaining a part of the variance that was already explained by the concurrent model.

To formally address this hypothesis, we used variance partitioning to isolate the unique contribution of each model to the group level RDM (Dwivedi et al., 2020; Groen et al., 2018; Hebart et al., 2018; Legendre, 2008). We conducted three linear regressions (one for each type of information separately and another one for both together) with model RDMs as predictors and the neural RDMs as predictands. Then, to infer the amount of unique variance explained by each model, we subtracted the explained variance of each single-model regression from the explained variance of the multi-model regression (Fig. 4C). As expected, the concurrent model uniquely explained a significant portion of the variance in both ROIs across both trial conditions (see Fig. 4D; average explained portion on episodic trials, V1 = .061, V2 = .042, both ps<.001; average explained portion on semantic trials, V1 = .134, V2 = .079 =, both ps<.001). More importantly, once the variance explained by the concurrent model was accounted for, the mnemonic model was still able to explain a significant portion of the remaining variance in EVC for episodic trials (average explained portion on episodic trials, V1 = .026, V2 = .021, both ps<.001). In contrast, for semantic trials, the memory model was unable to capture any variance that was not already explained by the concurrent model (average explained portion on semantic trials, V1 = .007, V2 = .004 =, both p>.05). Taken together, the variance partitioning result confirmed that, when accounting for the contribution of concurrent information, feedback predictions to occluded regions of EVC contain mnemonic information when the information was accessed episodically. This was not the case when the information was retrieved semantically. Importantly, while our results show that a concurrent vs. mnemonic parcellation can be performed on feedback signals, concurrent information is very likely to be in turn a mixture of low-level perceptual features (e.g., lines and colors, etc.), mid-level categorical information (e.g., kitchen as a general context) and even image-specific attentional patterns (Peelen and Kastner, 2014; Stokes et al., 2012). Although this distinction cannot be addressed by the current study, our findings lay the groundwork for future studies to delineate the specific content levels within concurrent feedback signals in EVC.

It should be noted that the asymmetric pattern of results between episodic and semantic trials could be reflecting a lack of sensitivity to capture representational similarities in semantic trials with our current paradigm. It is possible that, even if there was actual reinstatement from semantic access, our current experimental or analytical implementation would not be able to find the corresponding brain signatures. To discard this possibility, we used a new ROI that was not part of the registered analysis plan. Since our target memories were cartoon versions of real-world objects, we selected an ROI in the occipital cortex that has been shown to be critically involved in object processing, namely the object-selective cortex (LOC; (Grill-Spector et al., 2000)). We created an RDM in LOC following the same procedure as for V1 and V2, and computed an object-specific reinstatement index for each participant. The index was computed by subtracting the dissimilarity measures of *different room-same object* trials from those of *different room-different object* trials (Fig. 5A). Since this index is computed directly from distance measures in the RDMs, it has a straightforward interpretation in terms of representational change: any above zero value indicates that the retrieval of the same object from two different rooms increased the representational similarity in that ROI. Note that as occlusion is not effective for LOC, the computation of this index could theoretically reflect some high-order regularities across rooms. However, this is very unlikely to have a meaningful impact in practice as the specific scenes included different objects and these were counterbalanced across objects, retrieval conditions and participants. The analysis revealed significant object reinstatement in LOC for both episodic and semantic trials (both ps<.001), thus suggesting that objects retrieved semantically as well as episodically were represented in LOC. Moreover, we did not find differences in the index between trial conditions, z=0.638, p=.523 (two-sided Wilcoxon test), with modest evidence for the absence of a true effect BF10 = .35 (two-sided Bayesian t test), thus suggesting that object reinstatement in LOC was equivalent in both episodic and semantic conditions.

To compare LOC and EVC results more easily, we extended this index to the occluded portions of V1 and V2. As can be seen in Fig. 5B, and in line with the variance partitioning results, we observed object reinstatement in occluded V1 and V2 for the episodic condition (V1: average index value = .125, z=4.65, V2: average index value = .115, z=4.69, ps<.001). In contrast, there was no reinstatement in either ROI for semantic trials (V1: average index value = -.05, z=-3.84, V2: average index value = -.01, z=-1.70, ps>.05). We submitted the object reinstatement indices to a repeated-measures ANOVA with ROI (i.e., LOC, V1 and V2) and trial type (i.e., episodic and semantic) as within-participants factors to quantitatively describe this comparison. We observed a main effect of both ROI and trial type, F(2,56)=48,039, p<.001 and F(1,28)=62,447, p<.001, respectively. More interestingly, the significant interaction, F(2,56)=47,963, p<.001, further supported the observation above, namely that participants were able to access and represent in LOC the objects retrieved under both trial types. However, only episodically retrieved information reached the EVC as a feedback signal (Fig. 5B and see also *Supplementary Materials* for tests of spatial specificity on the fovea ROIs).

3.2. Different potential sources for feedback signals during semantic and episodic trials

Our results thus far have showed that memory content can inform feedback signals in the EVC depending on whether this content is episodically or semantically accessed. To shed light on this differentiation, we postulated that the two routes should rely on different neural computations and brain structures (Binder et al., 2009; Rosenbaum et al., 2016) as sources for the long-term representations that were fed back to lower levels (Barron et al., 2020). To locate these potential source regions, we planned a classification-based approach following previous reports relating EVC with distant brain regions (Bosch et al., 2014), with hippocampus and ventromedial prefrontal cortex as our candidate regions for episodic and semantic trials, respectively. However, the analysis above revealed that our SVMs were learning only concurrent information, thus making this analysis uninformative. Instead, we conducted a whole-brain PPI analysis (Friston et al., 1997), which can uncover modulations of effective connectivity between two brain regions as a function of a psychological variable. This analysis included the two retrieval

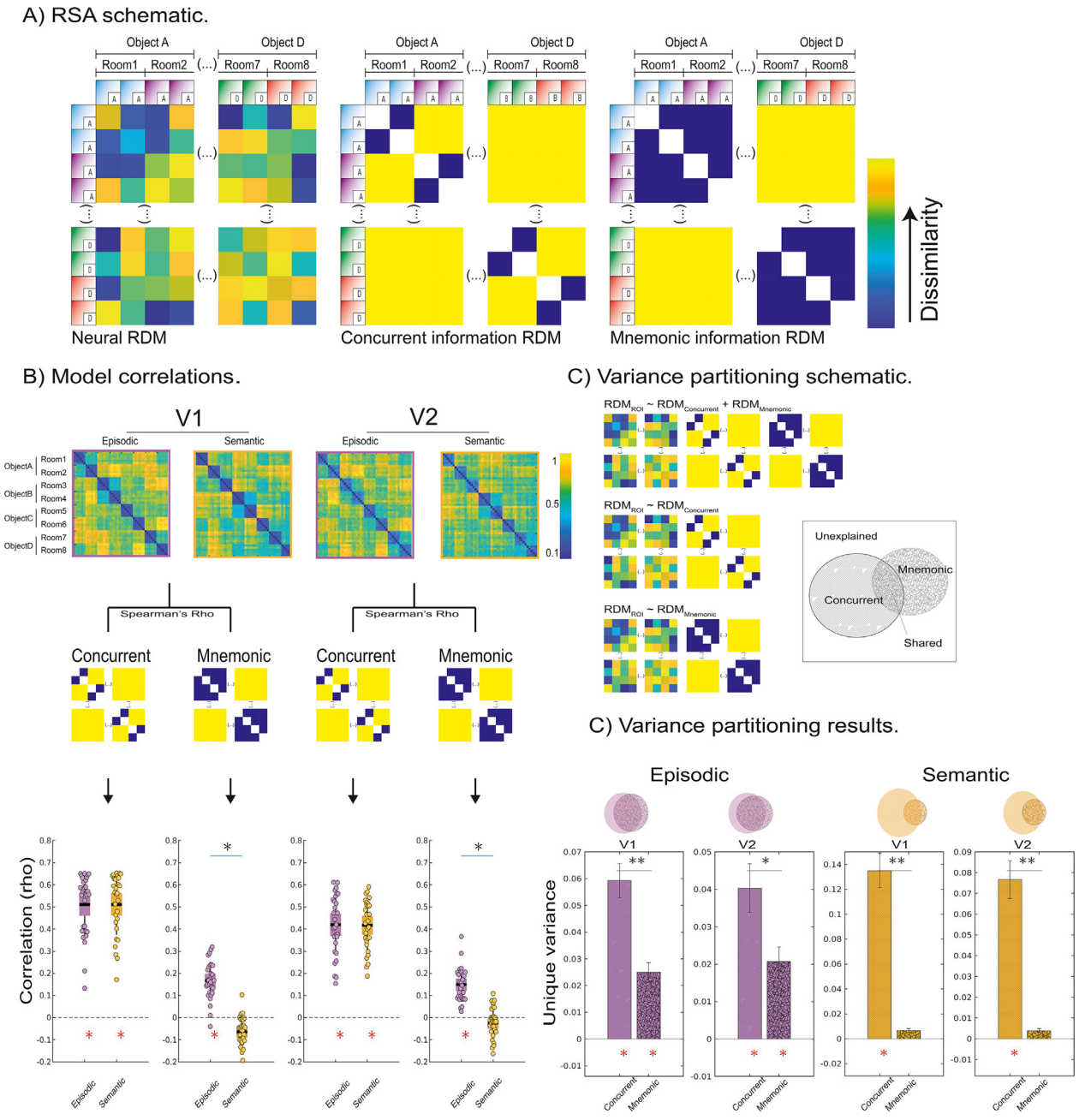

Fig. 4. Representational Similarity Analysis in occluded regions of the EVC. (a) Schematic depicting of how neural RDMs (of different ROIs) and model RDMs were constructed. Every RDM included a simplified representation of the stimuli as column and row headers. Every object (depicted with letters here) featured in two different rooms (depicted with colour of the background in the schematic stimuli) and was repeated six times. Note that for the sake of simplicity, only two objects and two repetitions are shown, rather than the four objects and six repetitions of the actual experiment. For neural RDMs, cross-nobis distances were computed for every pair of trials separately for episodic and semantic retrievals; for the concurrent RDM, minimal values (blue) were used for same-room trials and maximal values (yellow) for different-room trials; for the mnemonic RDM, minimal values (blue) were used for same-object and maximal values (yellow) for different-object trials. (b) Each model RDM was correlated with the ROI RDMs for episodic and semantic trials. Group averaged RDMs are shown in the top row; object names label the six repetitions of each object in a given room. Note that whereas the true diagonal is uninformative in these figures, a substructure clustering trials with the same rooms is evident to visual inspection; this substructure reflects the presence of concurrent information in occluded areas (confirmed by the model correlations in the bottom row). In the bottom row, each dot represents one participant and average scores are shown in black; red asterisks indicate correlations significantly different from zero ($p<.05$); black asterisks indicate significant differences between episodic and semantic trials ($p<.05$). Box whiskers represent +-1 standard error of the mean. (c) Schematic representation of the variance partitioning analysis. Three regression models were fitted with the ROI RDM as the predictand and the different models as predictors. The first regression (top panel) included both models as predictors, the second and third regressions included only one of the models (middle and bottom panels). The Venn diagram depicts the rationale of the variance partitioning analysis for the concurrent and the mnemonic models. (d) Variance partitioning results for episodic and semantic trials. The colour and the pattern of the bars denote the retrieval type and the model tested, respectively. Red asterisks indicate non-zero uniquely explained variance ($p<.05$); black asterisks indicate significant differences in the amount of explained variance by each model (* = $p<.05$; ** = $p<.001$). Note that, when the variance explained by the concurrent model was removed, the mnemonic model was only able to explain a significant portion of variance for episodic but not for semantic trials. Error bars represent +-1 standard error of the mean.

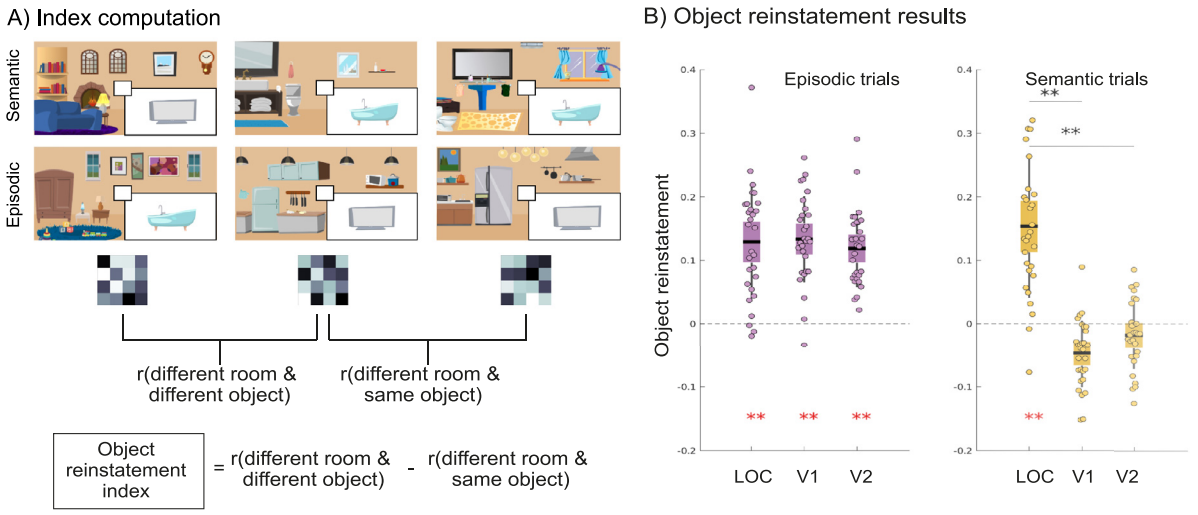

Fig. 5. Object-specific reinstatement index. (a) An object-specific reinstatement index was computed by assessing the average dissimilarity between same-object pairs (rightmost pair) and subtracting it from the average dissimilarity between different-object pairs (leftmost pair). Non-zero values in this index represent an increase in similarity during the retrieval of the same object. (b) Object reinstatement in visual cortex ROIs. Red asterisks indicate significant object reinstatement (<.05); black asterisks indicate significant differences in the amount of reinstatement in each ROI (* = p<.05; ** = p<.001). While object reinstatement was similar in LOC for both episodic and semantic retrievals, in V1 and V2 we saw object reinstatement only in episodic but not semantic trials.

conditions as main psychological modulators of effective connectivity. Although our pre-registered plan included the EVC ROIs as seed regions, the lack of object reinstatement in semantic trials would obscure the interpretation of any potential finding. Therefore, since we were able to measure object reinstatement in LOC for both memory conditions, we selected LOC as the seed region to be able to establish a fair comparison (see *Supplementary Text* for planned analysis with V1). As can be seen in Fig. 6, the results of this analysis revealed increased effective connectivity between LOC and a cluster in the right posterior parietal cortex during episodic trials (cluster corrected, voxel threshold $z > 3.1$, cluster threshold $p<.05$). In contrast, semantic trials increased functional coupling between LOC and fusiform gyrus ($p<.05$, cluster corrected; see *Supplementary Table* S2 for a summary of all clusters with increased connectivity). Since PPI does not allow directional inferences, and the pattern of regions observed was not anticipated, we restrict our interpretations to a differential pattern of connectivity for our two memory conditions. The observation that LOC differed in its effective connectivity with distant brain regions as a function of retrieval type supports the notion that episodic and semantic trials required qualitatively different cognitive operations to access the same information (i.e., the target objects). The extent to which these different operations are causally responsible for the lack of reinstatement in EVC during semantic trials will need to be explored in future studies.

4. Discussion

Our study characterizes the content of feedback signals by (1) replicating previous findings of feedback predictions in occluded portions of V1 and V2 and extending them to minimalistic stimuli which allow for careful control of low and high level features, (2) revealing that these feedback predictions can simultaneously represent information about the current surrounding context and mnemonic content that was formed in the past, (3) uncovering that the extent to which mnemonic information is fed down to EVC critically depends on the access mode for that information, and (4) showing that episodic and semantic access differentially engage dorsal (posterior parietal cortex) and ventral (fusiform gyrus) brain regions, respectively. While in predictive processing models priors are often assumed to be based on acquired knowledge about low-level features (e.g., line orientations; (Rao and Ballard, 1999b)), here we showed that higher-order mnemonic information can inform feedback signals as well in a nuanced way (Muckli et al., 2015; Quek and Peelen, 2020; Rademaker et al., 2019; Smith and Muckli, 2010). These results bring together predictive processing and memory systems, two major fields in cognitive neuroscience that are in principle closely related but are often considered in isolation.

4.1. Feedback signals carry different informational content

Occlusions happen constantly in our daily life and achieving object recognition from partially occluded inputs is one of the challenges that our perceptual system needs to overcome. In addition, perceptual disambiguation is not restricted to partial occlusions, since any perceptual experience can be understood as a form of probabilistic inference about the most likely stimuli to have caused the input (Bar, 2004; Von Helmholtz, 1866). In order to efficiently and accurately disambiguate sensory inputs, our brains need to integrate contextual information with pre-existing knowledge. Previous studies have successfully shown mnemonic information being replayed in EVC in the absence of a meaningful stimulation (i.e., in front of a blank display (Albers et al., 2013; Rademaker et al., 2019; Rahnev et al., 2011; Wimber et al., 2015)). Here, we extended these results by showing that mnemonic information is also present when the visual cortex is actively engaged in perception. Moreover, we show that during perception, mnemonic information coexists also with contextual information that is fed back from other early visual areas (in our paradigm, the non-occluded areas), presumably via lateral connections. The coexistence of concurrent and time-distant information enables the disambiguation of perceptual inputs and prevents inappropriate inferences drawn exclusively from memory. A rather ambiguous input (e.g., a drill in a poorly lit basement) can be clarified based on its surrounding information (e.g., it is placed on a workshop table next to other tools; (Bar, 2004; Quek and Peelen, 2020; Serences, 2016; Torralba, 2003)) and/or from memories of previous experiences (e.g., the last time you used it in your basement; (de Lange et al., 2018; Press et al., 2020)). Here we show that both types of information can coexist in time and place (Bar, 2004; Rademaker et al., 2019; Von Helmholtz, 1866).

In line with this idea, a recent study by Rademaker et al. (2019) showed that single-feature content held in working memory

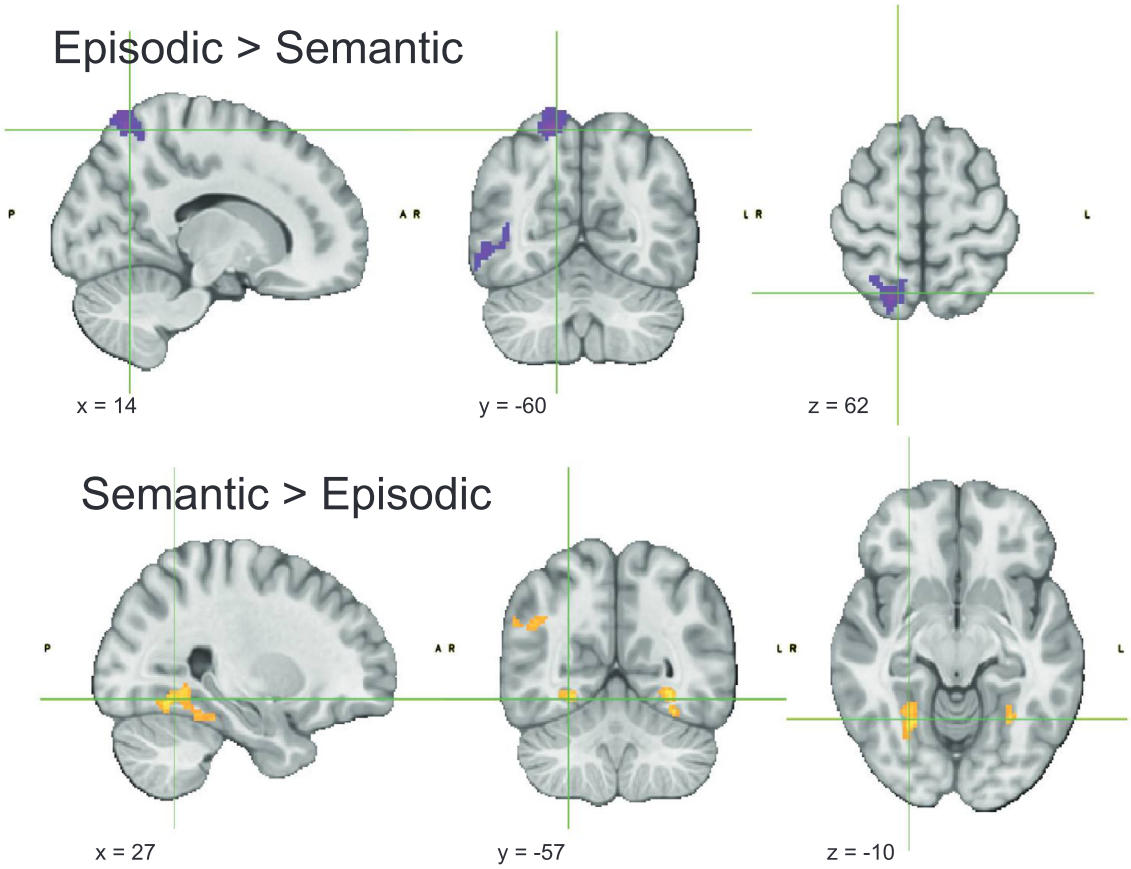

Fig. 6. Relating activity in distant brain regions to feedback signals. Whole-brain PPI analysis with LOC as seed region and retrieval type as psychological variable. The results revealed increased effective connectivity between LOC and right posterior parietal cortex during episodic trials and between LOC and bilateral fusiform for semantic trials.

(i.e., line orientation in a delayed-match-to-sample task) can be found in EVC. Interestingly, the disruption of the replayed pattern was mirrored by a decline in behavioral performance thus supporting the notion that feedback signals are causally involved in visual perception. Our results are compatible with the findings of Rademaker et al. and critically extend them by including content from consolidated episodic memories which are highly dimensional and naturalistic.

Several previous reports of top-down influences in EVC could also be interpreted as some form of concurrent information (Harrison et al., 2007; Lawrence et al., 2019; Morgan et al., 2019; Muckli et al., 2015; Quek and Peelen, 2020; Smith and Muckli, 2010). However, without jointly controlling for previous knowledge and incoming sensory inputs, it is difficult to disentangle the relative contribution of concurrent and time-distant information. In contrast, the present study was able to analytically quantify the amount of contextual and mnemonic information modulating activity in EVC. Rather than removing mnemonic or concurrent influences by using aseptic stimuli (Kok et al., 2020; Kok and Turk-Browne, 2018; Rademaker et al., 2019) or empty displays (Bosch et al., 2014; Stokes et al., 2009, 2012), our approach relied on RDMs to capture the different sources of modulation at the analysis stage (Kriegeskorte et al., 2008b; Nastase et al., 2020). By doing so, we showed that concurrent information biases activity in EVC more strongly than mnemonic information does, even when both are available: a result that was initially obscured by the SVM analyses. Therefore, our study also showcases the highly informative value of approaches relying on representational similarity with respect to classification-based methods when different sources of information are expected in the same brain region coinciding in time.

4.2. Feedback signals stemming from semantic and episodic access differ in content and neural substrates

Following Tulving's seminal definition, episodic memories are thought to be richer in perceptual details than semanticised memories which, by means of abstraction, have lost representational distinctiveness in favour of generalizability (Binder et al., 2009; Rosenbaum et al., 2016; Tulving, 1985). Here we show that the reinstatement of an object's representational pattern, under both episodic and semantic trials, took place in higher visual regions, namely LOC. The pattern is different in V1 and V2. That is, during episodic trials the object-specific pattern was successfully reinstated in non-stimulated subregions of V1 and V2; in contrast, there was no (consistent) reinstatement during semantic trials.

Our experimental design was set up to ensure that the set of target objects for the episodic and semantic trials was identical and that the object that should be retrieved for each trial was non-ambiguous. The exact location of each object was kept the same across the two different rooms they were assigned to during the pre-training phase. By this, during semantic trials, participants were likely to mentally represent the objects at the same spatial location in the occluded area. These features rendered the semantic and episodic trials to be as comparable as possible, other than how the information was accessed. However, it is possible that reinstatement in the episodic trials was still more perceptually precise (e.g., higher spatial precision) than in semantic trials because the retrieval was based on associative memory of the experienced event. To provide tentative support for this idea, we ran additional exploratory analysis further decomposing the mnemonic variance

of episodic trials into two low-level components. Namely, position- and colour-based information (see *Supplementary Text* and Fig. S3). The result of this analysis shows that the mnemonic modulation of feedback signals is compatible with a reinstatement of the low-level characteristics of our stimuli. Hence, our interpretation is that the EVC is not representing object identity detached from its low-level characteristics. Rather, it is re-instantiating (through feedback signals) the features of the experienced events (e.g., position, color, frequency, etc.). Given that episodic memories tend to contain more perceptual information, their retrievals are more likely to drive reinstatement and feedback in early visual areas than semantic ones. To test this postulation, future studies with episodic retrievals containing unprecise spatial information are needed.

Complementing the observed asymmetric reinstatement of memory content in EVC, our connectivity results indicate that semantic and episodic retrievals rely on different brain networks. The posterior parietal cortex is considered to be part of a wider hippocampal memory network, which is particularly engaged when accessing temporally bound memories (Vincent et al., 2006). In addition, subdivisions of the posterior parietal cortex have been shown to be recruited during the retrieval of specific detailed-rich memories but not of merely familiar ones (Silson et al., 2019). On the other hand, while semantic representations are assumed to be widely distributed over the cortex, activity in some regions such as the fusiform gyrus has been related to semantic tasks involving object selection (Rogers et al., 2021), categorization (Binder et al., 2009), and non-specific recognition memory (Garoff et al., 2005). Moreover, subregions of the fusiform gyrus have also been related to the representation of abstract concepts detached from low-level features (Tsantani et al., 2021). The requirements of our task closely mimic these processes. In episodic trials, participants accessed the unique room-object combinations learned in the study session to retrieve the appropriate object; in semantic trials, to retrieve the appropriate object, participants had to correctly identify the room category shown (e.g., bathroom) and mentally select the semantically fitting object (e.g., a bathtub) among four possible candidates. Accordingly, our results revealed that effective connectivity between LOC and the posterior parietal cortex was enhanced during the episodic retrieval of room-object pairs. In contrast, we observed that LOC changed its functional coupling from dorsal to ventral regions (i.e., fusiform gyrus) during semantic retrievals. This last finding, together with the lack of EVC reinstatement for semantic retrievals, is in line with previous work relating activity in the left fusiform to gist-like recognition memory (Garoff et al., 2005; Tsantani et al., 2021). Due to the lack of directionality in PPI analysis, we cannot ascertain whether LOC was modulated by distant activity or vice versa. However, the differential crosstalk between an area engaged in active object reinstatement and a set of memory-related networks is compatible with the idea that top-down predictions stem from different higher-order (memory) representations.

It is important to note that our episodic and semantic trials do not unequivocally refer to the access of pure episodic and semantic memory *traces*. On the one hand, using real-world stimuli makes it impossible to entirely avoid their inherent semantic information. On the other hand, as the semantically retrieved objects were studied on the previous day, these carried substantial episodic information. We acknowledge that these issues preclude the interpretation of our results as absolute differences between episodic and semantic representations, but rather as relative differences supported by the differential pattern of results between conditions. Moreover, our episodic and semantic conditions also differed regarding room-to-object congruency and familiarity with the room images (see Methods section on the rationale for this). However, and critically, during the occlusion task, the information that was actually accessed (i.e., the objects) was the same for both memory conditions. That is, during both types of trials participants had to access one object among the same four objects studied the previous day. This equates exposure of the to-be-retrieved information across memory conditions, thus ruling out the interpretations based on stimulus familiarity.

Therefore, we would rather interpret our results in relation to the operations through which the content was accessed (Cowell et al., 2019). In particular, the environment may prompt the access of object representations through semantic or episodic routes, and the operations needed in each situation would be different. For instance, entering the office where you saw a colleague the day before will trigger episodic remembering of her face. However, if you know that your colleague switched offices, entering her new office will still trigger the memory of your colleague's face even if you have never visited that office before. In this latter case, remembering of her face will be accessed via a semantic route, which links the concept of office and the knowledge of the switch to his face. We argue that episodic and semantic trials in our task require the use of different operations, which is supported by the observed differential pattern of connectivity between dorsal and ventral regions, respectively. In addition, the episodic access from the previous day would contain a wide variety of precise low-level features (e.g., where her desk was) which the semantic access would not.

Several previous studies exploring EVC activation in the absence of external stimuli did so in the context of mental imagery (Albers et al., 2013; Kosslyn et al., 1995; Kosslyn and Thompson, 2003; Stokes et al., 2009). In addition, the relationship between mental imagery and memory has been the focus of research for a long time (Albers et al., 2013; Slotnick et al., 2011). In our paradigm, the task participants were performing closely resembles those traditionally used for mental imagery (i.e., to vividly visualize content that is not present) and indeed our results are compatible with previous imagery-based reports of top-down modulations in EVC. Therefore, instead of drawing a rather artificial hard boundary between imagery and memory retrieval, we argue that the top-down influence of both constructs relies on a common implementation mechanism (i.e., feedback signals) informed by mnemonic content. This is in line with the "dynamic blackboard" idea which considers that the EVC can be recruited for top-down modulations stemming from internal models, regardless of whether these are either imagery- or memory-based, (Albers et al., 2013; Bullier, 2001; Slotnick et al., 2011).

Finally, a full characterization of the nature of feedback signals across the visual hierarchy would need to eventually include all the visual regions between LOC and V1. In the current study, we mainly focus on the very early visual regions (V1 and V2), but our paradigm sets the basis for an exhaustive exploration of the feedback content in the rest of the visual hierarchy. In addition, our analysis approach would be rather equivalent to applying a conventional multivariate analysis of variance (e.g., canonical variance analysis) with a two-factor design — where the first factor would be object identity, and the second factor would be information type (concurrent versus mnemonic) Future studies extending our paradigm to other visual regions and replicating our results with different analysis pipelines would enable such full characterization.

Taken together, our findings shed light on the role that memory plays in generating predictions. The retrieval of pre-existing information can serve as a source mechanism to inform visual prediction. Here we show that during active perception, feedback signals carry information about the contextual surrounding and about long-term (episodic) memories. It is this coexistence in space and time that sets the basis for the integration of sensory inputs, situational information, and previous knowledge (Friston, 2005; Rao and Ballard, 1999a; Stokes et al., 2012). However, our study did not fully resolve how such integration takes place neurally (Mumford, 1992; Rademaker et al., 2019; Rao and Ballard, 1999b; Stokes et al., 2009). Here, laminar-specifc fMRI of the EVC may provide key insights by uncovering layer-specific profiles for concurrent and mnemonic feedback information. Specifically, mnemonic information which presumably stems from higher-order structures may arrive at the deep layers, while concurrent information, presumably originated within nearby regions, may arrive at the superficial layers (Markov et al., 2013). In addition, whereas in this study we have focused on the earliest visual processing areas (i.e., V1 and V2), a further exhaustive delineation of all the subregions along the visual hierarchy could shed more light onto how this integration is instantiated at intermediate levels of

the hierarchy (e.g., V3; (Stokes et al., 2012)). Future studies combining high-field fMRI and our experimental approach have the potential to advance our understanding of how different sources of feedback information are integrated together with feedforward signals.

Data and code availability

- Stimulation analysis scripts: https://github.com/ortiztud/feedbes.
- Raw data: https://openneuro.org/datasets/ds003691.
- Unthresholded Z-maps from PPI: https://neurovault.org/collections/UAFOYKRZ/.

Funding sources

European Research Council Starting grant ERC-2018-StG-PIVOTAL-758898 (YLS). Jacobs Foundation Research Fellowship JRF 2018–2020 (YLS). German Research Foundation Project ID 327654276, SFB 1315, “Mechanisms and Disturbances in Memory Consolidation: From Synapses to Systems” (YLS). Goethe Research Academy for Early Career Researchers - Fokus A/B program (JO). Hessian Ministry of Higher Education, Science, Research and Art, “The Adaptive Mind” (YLS).

Declaration of Competing Interest

The authors declare no competing financial interests.

Credit authorship contribution statement

Javier Ortiz-Tudela: Conceptualization, Data curation, Formal analysis, Investigation, Methodology, Project administration, Software, Visualization, Writing – original draft, Writing – review & editing. **Johanna Bergmann:** Methodology, Writing – review & editing. **Matthew Bennett:** Methodology, Writing – review & editing. **Isabelle Ehrlich:** Data curation, Formal analysis, Investigation, Software, Visualization, Writing – review & editing. **Lars Muckli:** Methodology, Supervision, Writing – review & editing. **Yee Lee Shing:** Conceptualization, Funding acquisition, Methodology, Project administration, Supervision, Writing – review & editing.

Data availability

I have shared my data/code at the Attach file step.

Acknowledgments

We thank members of the LISCO lab (PI: YLS), Carlos Gonzalez-García, Catarina Sanches-Ferreira, and Francesco Pupillo for their helpful comments on this research.

Supplementary materials

Supplementary material associated with this article can be found, in the online version, at doi:10.1016/j.neuroimage.2022.119778.

References

Abdulrahman, H., Henson, R.N., 2016. Effect of trial-to-trial variability on optimal event-related fMRI design: implications for Beta-series correlation and multi-voxel pattern analysis. Neuroimage doi:10.1016/j.neuroimage.2015.11.009.

Albers, A.M., Kok, P., Toni, I., Dijkerman, H.C., De Lange, F.P., 2013. Shared representations for working memory and mental imagery in early visual cortex. Curr. Biol. 23 (15), 1427–1431. doi:10.1016/J.CUB.2013.05.065.

Animaker. (n.d.). Retrieved August 13, 2018, from https://www.animaker.com/

Bar, M., 2004. Visual objects in context. Nat. Rev. Neurosci. 5 (8), 617–629. doi:10.1038/nrn1476.

Barron, H.C., Auksztulewicz, R., Friston, K., 2020. Prediction and memory: a predictive coding account. Prog. Neurobiol. doi:10.1016/j.pneurobio.2020.101821, April..

Binder, J.R., Desai, R.H., Graves, W.W., Conant, L.L., 2009. Where is the semantic system? A critical review and meta-analysis of 120 functional neuroimaging studies. Cereb. Cortex doi:10.1093/cercor/bhp055.

Bosch, S.E., Jehee, J.F.M., Fernández, G., Doeller, C.F., 2014. Reinstatement of associative memories in early visual cortex is signaled by the hippocampus. J. Neurosci. 34 (22), 7493–7500. doi:10.1523/JNEUROSCI.0805-14.2014.

Bullier, J., 2001. Feedback connections and conscious vision. Trends Cogn. Sci. 5 (9), 369–370. doi:10.1016/S1364-6613(00)01730-7.

Clark, A., 2013. Whatever next, Predictive brains, situated agents, and the future of cognitive science. Behav. Brain Sci. 36 (3), 181–204. doi:10.1017/S0140525X12000477.

Cowell, R.A., Barense, M.D., Sadil, P.S., 2019. A roadmap for understanding memory: Decomposing cognitive processes into operations and representations. eNeuro 6 (4), 1–19. doi:10.1523/ENEURO.0122-19.2019.

de Lange, F.P., Heilbron, M., Kok, P., 2018. How do expectations shape perception?. In: Trends in Cognitive Sciences, 22. Elsevier Ltd, pp. 764–779. doi:10.1016/j.tics.2018.06.002.

Dwivedi, K., Martin Cichy, R., Roig, G., 2020. Unravelling representations in scene-selective brain regions using scene parsing deep neural networks. J. Cogn. Neurosci. 1–12. doi:10.1101/2020.03.10.985309.

Esteban, O., Markiewicz, C.J., Blair, R.W., Moodie, C.A., Isik, A.I., Erramuzpe, A., Kent, J.D., Goncalves, M., DuPre, E., Snyder, M., Oya, H., Ghosh, S.S., Wright, J., Durnez, J., Poldrack, R.A., Gorgolewski, K.J., 2019. fMRIPrep: a robust preprocessing pipeline for functional MRI. Nat. Methods 16 (1), 111–116. doi:10.1038/s41592-018-0235-4.

Friston, K., 2005. A theory of cortical responses. Philos. Trans. R. Soc. B Biol. Sci. doi:10.1098/rstb.2005.1622.

Friston, K., Buechel, C., Fink, G.R., Morris, J., Rolls, E., Dolan, R.J., 1997. Psychophysiological and modulatory interactions in neuroimaging. Neuroimage 6 (3), 218–229. doi:10.1006/nimg.1997.0291.

Garoff, R.J., Slotnick, S.D., Schacter, D.L., 2005. The neural origins of specific and general memory: the role of the fusiform cortex. Neuropsychologia 43 (6), 847–859. doi:10.1016/J.NEUROPSYCHOLOGIA.2004.09.014.

Grill-Spector, K., Kushnir, T., Hendler, T., Malach, R., 2000. The dynamics of object-selective activation correlate with recognition performance in humans. Nat. Neurosci. doi:10.1038/77754.

Groen, I.I.A., Greene, M.R., Baldassano, C., Fei-Fei, L., Beck, D.M., Baker, C.I., 2018. Distinct contributions of functional and deep neural network features to representational similarity of scenes in human brain and behavior. eLife 7. doi:10.7554/ELIFE.32962.

Harrison, L.M., Stephan, K.E., Rees, G., Friston, K.J., 2007. Extra-classical receptive field effects measured in striate cortex with fMRI. Neuroimage 34 (3), 1199–1208. doi:10.1016/J.NEUROIMAGE.2006.10.017.

Hebart, M.N., Bankson, B.B., Harel, A., Baker, C.I., Cichy, R.M., 2018. The representational dynamics of task and object processing in humans. eLife 7. doi:10.7554/ELIFE.32816.

Hebart, M.N., Görgen, K., Haynes, J.D., 2015. The decoding toolbox (TDT): A versatile software package for multivariate analyses of functional imaging data. Front. Neuroinform. doi:10.3389/fninf.2014.00088.

Kok, P., Rait, L.I., Turk-Browne, N.B., 2020. Content-based dissociation of hippocampal involvement in prediction. J. Cogn. Neurosci. 32 (3), 527–545. doi:10.1162/jocn_a_01509.

Kok, P., Turk-Browne, N.B., 2018. Associative prediction of visual shape in the hippocampus. J. Neurosci. 38 (31), 6888–6899. doi:10.1523/JNEUROSCI.0163-18.2018.

Kosslyn, S.M., Thompson, W.L., 2003. When is early visual cortex activated during visual mental imagery? Psychol. Bull. 129 (5), 723–746. doi:10.1037/0033-2909.129.5.723.

Kosslyn, S.M., Thompson, W.L., Klm, I.J., Alpert, N.M., 1995. Topographical representations of mental images in primary visual cortex. Nature 378 (6556), 496–498. doi:10.1038/378496a0, 1995 378:6556.

Kriegeskorte, N., Mur, M., Bandettini, P., 2008a. Representational similarity analysis - connecting the branches of systems neuroscience. Front. Syst. Neurosci. doi:10.3389/neuro.06.004.2008.

Kriegeskorte, N., Mur, M., Bandettini, P., 2008b. Representational similarity analysis - connecting the branches of systems neuroscience. Front. Syst. Neurosci. 2, 1–28. doi:10.3389/neuro.06.004.2008, NOV.

Lawrence, S.J.D., Norris, D.G., De Lange, F.P., 2019. Dissociable laminar profiles of concurrent bottom-up and top-down modulation in the human visual cortex. eLife 8. doi:10.7554/ELIFE.44422.

Legendre, P., 2008. Studying beta diversity: ecological variation partitioning by multiple regression and canonical analysis. J. Plant Ecol. doi:10.1093/jpe/rtm001.

Markov, N.T., Ercsey-Ravasz, M., Van Essen, D.C., Knoblauch, K., Toroczkai, Z., Kennedy, H., 2013. Cortical high-density counterstream architectures. Science 342 (6158). doi:10.1126/science.1238406, American Association for the Advancement of Science.

Morgan, A.T., Petro, L., Muckli, L., 2016. Cortical feedback to V1 and V2 contains unique information about high-level scene structure. J. Vis. doi:10.1167/16.12.529.

Morgan, A.T., Petro, L.S., Muckli, L., 2019. Scene representations conveyed by cortical feedback to early visual cortex can be described by line drawings. J. Neurosci. doi:10.1523/JNEUROSCI.0852-19.2019.

Muckli, L., De Martino, F., Vizioli, L., Petro, L.S., Smith, F.W., Ugurbil, K., Goebel, R., Yacoub, E., 2015. Contextual Feedback to Superficial Layers of V1. Curr. Biol. doi:10.1016/j.cub.2015.08.057.

Mumford, D., 1992. On the computational architecture of the neocortex. Biol. Cybern. 66 (3), 241–251. doi:10.1007/BF00198477, 1992 66:3.

Mumford, J.A., Turner, B.O., Ashby, F.G., Poldrack, R.A., 2012. NeuroImage Deconvolving BOLD activation in event-related designs for multivoxel pattern classi fi cation analyses. Neuroimage 59 (3), 2636–2643. doi:10.1016/j.neuroimage.2011.08.076.

Nastase, S.A., Goldstein, A., Hasson, U., 2020. Keep it real: rethinking the primacy of experimental control in cognitive neuroscience. Neuroimage 222, 117254. doi:10.1016/J.NEUROIMAGE.2020.117254.

Peelen, M.V., Kastner, S., 2014. Attention in the real world: toward understanding its neural basis. Trends Cogn. Sci. doi:10.1016/j.tics.2014.02.004.

Press, C., Kok, P., Yon, D., 2020. The perceptual prediction paradox. Trends Cogn. Sci. 24 (1), 13–24. doi:10.1016/j.tics.2019.11.003, Elsevier Ltd..

Quek, G.L., Peelen, M.V., 2020. Contextual and spatial associations between objects interactively modulate visual processing. Cereb. Cortex 30 (12), 6391–6404. doi:10.1093/CERCOR/BHAA197.

Rademaker, R.L., Chunharas, C., Serences, J.T., 2019. Coexisting representations of sensory and mnemonic information in human visual cortex. Nat. Neurosci. 22 (8), 1336–1344. doi:10.1038/s41593-019-0428-x.

Rahnev, D., Lau, H., de Lange, F.P., 2011. Prior expectation modulates the interaction between sensory and prefrontal regions in the human brain. J. Neurosci. 31 (29), 10741–10748. doi:10.1523/JNEUROSCI.1478-11.2011.

Rao, R.P.N., Ballard, D.H., 1999a. Hierarchical predictive coding model hierarchical predictive coding of natural images. Nat. Neurosci. 2, 79–87.

Rao, R.P.N., Ballard, D.H., 1999b. Predictive coding in the visual cortex: a functional interpretation of some extra-classical receptive-field effects. Nat. Neurosci. 2 (1), 79–87. doi:10.1038/4580, 1999 2:1.

Ritchey, M., Cooper, R.A., 2020. Deconstructing the posterior medial episodic network. Trends Cogn. Sci. 24 (6), 451–465. doi:10.1016/J.TICS.2020.03.006.

Rogers, T.T., Hocking, J., Mechelli, A., Patterson, K., Price, C., 2021. Fusiform activation to animals is driven by the process, not the stimulus. J. Cogn. Neurosci. 17 (3), 434–445.

Rosenbaum, R.S., Kim, A.S.N., Baker, S., 2016. Episodic and semantic memory. The Curated Reference Collection in Neuroscience and Biobehavioral Psychology doi:10.1016/B978-0-12-809324-5.21037-7.

Serences, J.T., 2016. Neural mechanisms of information storage in visual short-term memory. Vis. Res. 128, 53–67. doi:10.1016/J.VISRES.2016.09.010.

Silson, E.H., Steel, A., Kidder, A., Gilmore, A.W., Baker, C.I., 2019. Distinct subdivisions of human medial parietal cortex support recollection of people and places. eLife 8. doi:10.7554/ELIFE.47391.

Slotnick, S. D., Thompson, W. L., & Kosslyn, S. M. (2011). Visual memory and visual mental imagery recruit common control and sensory regions of the brain. 3(1), 14–20. doi:10.1080/17588928.2011.578210.

Smith, F.W., Muckli, L., 2010. Nonstimulated early visual areas carry information about surrounding context. Proc. Natl. Acad. Sci. USA doi:10.1073/pnas.1000233107.

Spunt, B. (2016). easy-optimize-x: formal release for archiving on Zenodo. 10.5281/ZENODO.58616

Squire, L.R., 1998. Memory systems. C. R. Acad. Sci. III 321 (2), 153–156. doi:10.1016/S0764-4469(97)89814-9, -3.

Stelzer, J., Chen, Y., Turner, R., 2013. Statistical inference and multiple testing correction in classification-based multi-voxel pattern analysis (MVPA): Random permutations and cluster size control. Neuroimage 65, 69–82. doi:10.1016/j.neuroimage.2012.09.063.

Stokes, M.G., Atherton, K., Patai, E.Z., Nobre, A.C., 2012. Long-term memory prepares neural activity for perception. Proc. Natl. Acad. Sci. USA 109 (6), E360–E367. doi:10.1073/pnas.1108555108.

Stokes, M.G., Thompson, R., Cusack, R., Duncan, J., 2009. Top-down activation of shape-specific population codes in visual cortex during mental imagery. J. Neurosci. 29 (5), 1565–1572. doi:10.1523/JNEUROSCI.4657-08.2009.

Torralba, A., 2003. Contextual priming for object detection. Int. J. Comput. Vis. 53 (2), 169–191. doi:10.1023/A:1023052124951, 2003 53:2.

Tsantani, M., Kriegeskorte, N., Storrs, K., Williams, A.L., McGettigan, C., Garrido, L., 2021. Ffa and ofa encode distinct types of face identity information. J. Neurosci. 41 (9). doi:10.1523/JNEUROSCI.1449-20.2020.

Tulving, E., 1985. How many memory systems are there? Am. Psychol. doi:10.1037/0003-066x.40.4.385.

Tulving, E., Markowitsch, H.J., 1998. Episodic and declarative memory: role of the hippocampus. Hippocampus doi:10.1002/(SICI)1098-1063, (1998)8:3<198::AID-HIPO2>3.0.CO;2-G.

Vincent, J.L., Snyder, A.Z., Fox, M.D., Shannon, B.J., Andrews, J.R., Raichle, M.E., Buckner, R.L., 2006. Coherent spontaneous activity identifies a hippocampal-parietal memory network. J. Neurophysiol. 96 (6), 3517–3531. doi:10.1152/jn.00048.2006.

Von Helmholtz, H. (1866). Concerning the Perceptions in General J. Southall (Ed.); 3rd ed.). New York, Dover Publications (translation).

Williams, M.A., Baker, C.I., Op De Beeck, H.P., Mok Shim, W., Dang, S., Triantafyllou, C., Kanwisher, N., 2008. Feedback of visual object information to foveal retinotopic cortex. Nat. Neurosci. doi:10.1038/nn.2218.

Wimber, M., Alink, A., Charest, I., Kriegeskorte, N., & Michael, C. (2015). Retrieval induces adaptive forgetting of competing memories via cortical pattern suppression. 18(4), 582–589. 10.1038/nn.3973.Retrieval

Woolrich, M.W., Ripley, B.D., Brady, M., Smith, S.M., 2001. Temporal autocorrelation in univariate linear modeling of FMRI data. Neuroimage 14 (6), 1370–1386. doi:10.1006/nimg.2001.0931.

Yarkoni, T., Poldrack, R.A., Nichols, T.E., Van Essen, D.C., Wager, T.D., 2011. Large-scale automated synthesis of human functional neuroimaging data. Nat. Methods doi:10.1038/nmeth.1635.

Further reading

Brodoehl, S., Witte, O.W., Klingner, C.M., 2016. Measuring eye states in functional MRI. BMC Neurosci. 17 (1), 1–10. doi:10.1186/s12868-016-0282-7.

Thaler, L., Schütz, A.C., Goodale, M.A., Gegenfurtner, K.R., 2013. What is the best fixation target, the effect of target shape on stability of fixational eye movements. Vis. Res. 76, 31–42. doi:10.1016/j.visres.2012.10.012.